Electronic supplemental information

The active site architecture in peroxiredoxins: a case study for *Mycobacterium tuberculosis* AhpE

Brandán Pedre[a,b,c] Laura A. H. van Bergen [b,c,d], Anna Palló [a,b,c], Leonardo A. Rosado [a,b,c], Veronica Tamu Dufe [a,b,c], Inge Van Molle [a,b,c], Khadija Wahni [a,b,c], Huriye Erdogan [a,b,c], Mercedes Alonso [d], Frank De Proft[d] and Joris Messens [a,b,c]

[a.] *Structural Biology Research Center, VIB, 1050 Brussels, Belgium*
[b.] *Brussels Center for Redox Biology, 1050 Brussels, Belgium*
[c.] *Structural Biology Brussels, Vrije Universiteit Brussel, 1050 Brussels, Belgium*
[d.] *Research Group of General Chemistry, Vrije Universiteit Brussel, 1050 Brussels, Belgium*

Details of the experimental procedures

Expression and purification of MtAhpE variants

MtAhpE WT, F37H, T42V and R116A were expressed in *Escherichia coli* BL21 (DE3) (expression vector pDEST17) as a recombinant N-terminal His-tagged protein and purified as described[1].

Pre-treatment of MtAhpE variants

MtAhpE variants (WT, F37H, T42V, R116A) were reduced by incubation with 50 mM dithiotreitol for 30 min at 4˚C. Excess of dithiotreitol was removed by size-exclusion chromatography using a Superdex75 10/300 column (GE Healthcare), equilibrated in reaction buffer: 100 mM sodium phosphate pH 7.4, 100 µM diethylene triamine penta-acetic acid (DTPA).

Measurement of the H_2O_2 consumption over time

The direct H_2O_2 consumption rate by the MtAhpE variants was determined by the ferrous oxidation of xylenol orange (FOX). Reduced MtAhpE (100 µM) was mixed with 100 µM H_2O_2 in reaction buffer at 25˚C. After 20, 40, 60, 120, 240 seconds of reaction, 10 µL of the reaction was mixed with 490 µL of the FOX reaction mix (100 µM xylenol orange, 250 µM ammonium ferrous sulfate, 100 mM sorbitol and 25 mM H_2SO_4), and incubated for 30 min at room temperature in darkness. At the end of the reaction, absorbance at 560 nm was measured, and the H_2O_2 concentration was calculated based on a H_2O_2 standard curve.

pK_a determination of the peroxidatic cysteine

Reduced MtAhpE was generated as described above, whereas the iodoacetamide-alkylated sample (considered as the oxidized sample) was made by adding 10 molar excess iodoacetamide to reduced MtAhpE and incubated for 30 min at room temperature in the dark. The excess of dithiotreitol or iodoacetamide in each sample was removed on a Superdex75 10/300 column (GE Healthcare) equilibrated with a polybuffer: 10 mM sodium citrate, 10 mM sodium borate, 10 mM sodium phosphate, pH 8.5. The pH of the samples was stepwise decreased with HCl. For every pH decrease, the absorbance at 280 nm and 240 nm was recorded on a Cary100 Bio UV-visible spectrophotometer (Varian, Palo Alto, CA). The absorption at 240 nm was standardized with the absorption at 280 nm for each pH value ($A_{240\ nm}/A_{280\ nm}$) to compensate for the dilution caused by the addition of HCl. The corrected absorption $(A_{240}/A_{280})_{red}/(A_{240}/A_{280})_{ox}$ was plotted against the pH and fitted with the Henderson-Hasselbalch equation[2].

Determining the oxidation rate constant of MtAhpE mutants

This method is based on the decrease in the protein intrinsic fluorescence intensity upon enzyme oxidation by H_2O_2, as described[1]. Reduced MtAhpE (1 µM) was rapidly mixed with excess concentrations of H_2O_2 in reaction buffer and 25°C, using an Applied Photophysics SX-20 stopped-flow spectrofluorimeter (mixing time of ≤1.2 ms), following the total fluorescence intensity decrease (λ_{ex}= 295 nm, 320 nm cut-off filter). For the F37H mutant, the following H_2O_2 concentrations were used: 20, 30, 40, 50 and 60 µM. The observed rate constant was determined by fitting the first

phase of the progress curve to a single exponential equation (Fig. S2A). For the T42V mutant, the following H_2O_2 concentrations were used: 0.4, 0.8, 1.2, 1.6 and 2 mM. The observed rate constants were determined by fitting the first phase of the progress curve to a single exponential equation (Fig. S2B). For the R116A mutant, the following H_2O_2 concentrations were used: 5, 10, 15, 20 and 25 mM. The observed rate constants were determined by fitting the progress curves to a single exponential plus slope equation (Fig. S2C). From the plot of the observed rate constants versus H_2O_2 concentrations, the second-order rate constants for the reaction between the reduced MtAhpE and H_2O_2 at pH 7.4 and 25°C were calculated.
In this reaction, the thiolate of MtAhpE and the protonated peroxide are the reactive species. The pK_a value of H_2O_2 is 11.7, thus the peroxide will be protonated. The percentage of the thiolate form (y) in the MtAhpE variants was calculated using the following equation:

$$y = \frac{100}{1 + 10^{-(pH - pK_a)}}$$

The pH-independent rate constant of the MtAhpE variants was calculated by dividing the obtained rate constant at pH 7.4 by the percentage of the thiolate form at the same pH, obtained by this equation.

Crystallization, X-ray data collection, and structure determination
Crystals of MtAhpE R116A and F37H were grown using the hanging drop method at 20°C at 20 and 30 mg/ml, respectively, in 20 mM HEPES, 150 mM NaCl, pH 7.6 1.5 M Na-malonate, 0.1 M Na-acetate pH 4.5, and 0.2 M Na-citrate, 0.1 M Na-HEPES, 30% v/v (+/-)-2-methyl-2,4-pentane pH 7.5, respectively. Crystals were flash-cooled with liquid nitrogen. X-ray diffraction data were collected at 100K at beamline I03 of the Diamond synchrotron facility for MtAhpE R116A and at the Proxima 1 beamline of the Soleil synchrotron facility for MtAhpE F37H. Data were processed using XDS[3] and the structure was determined by molecular replacement using Phaser[4] and the re-refined reduced MtAhpE structure (PDB entry 4X0X) as a search model. Atomic coordinates were refined using REFMAC5[5] and manually inspected using COOT[6]. The structure was validated using MolProbity[7]. X-ray data collection parameters, processing and refinement statistics are summarized in Table S1. The refined structures and the corresponding structure factor amplitudes were deposited to the PDB under the accession code 4XIH for MtAhpE R116A and 5C04 for MtAhpE F37H.

Molecular Dynamics setup
All structures were modeled with the peroxidatic cysteine (C_P) as a thiolate (S^-), and hydrogens were added using CHARMM[8] version 37b1, with the all-atom CHARMM22 force field[9]. All structures were centered in a 35 Å sphere of TIP3P[10] water molecules with the sulfur of the cysteine at the center, No counter-ions were added as a fixed zone, after 25 Å was used obtaining a net charge of -5 for the WT, the F37H mutant and the T42V mutant, and -6 for the R116A mutant. The reaction zone was defined as a sphere of 21 Å from the center[11]. In the shell between 21 and 25 Å, the atoms were harmonically restrained with increasing constraints outwards at every Å. Beyond 25 Å, all atomic positions were kept constant. The water molecules were

energy-minimized, followed by a short heating step from 10K to 300K in 1 ps and an equilibration of 20 ps, and then a short second energy-minimization. From this, the whole structure was energy-minimized by
6, short, 500-step cycles of steepest descent minimization and by an adopted
basis Newton-Raphson minimization. The systems were heated gradually to 300K at the pace of 5K/ps, followed by 100 ps of equilibration. Subsequently, 30 ns of simulation were performed. Leapfrog Langevin dynamics were conducted with a time step of 1 fs, and all X-H bonds were constrained with the SHAKE algorithm[12]. All simulations were performed under constant temperature of 300K. Every 35 steps, the atoms were checked for being in the Langevin region of 21 Å. Energies of the system were recorded after every 100 steps, coordinates and velocities of the system were recorded after every 500 steps. The list of non-bonded interactions was updated based on a heuristic testing with a cut-off of 14 Å. Atom electrostatics were treated with the classical force shift method, and the van-der-Waals interaction forces and energies were set to zero at the cut-off distance using a shift method with 12 Å cut-off.

QM calculations

The positions for the model systems of the Cys-Thr and Cys-His complexes were taken from the equilibrated MD structures of the WT and F37H, respectively, with the cysteine modeled as a thiolate. All amino acids were modeled with the Cα as a CH_3-R, in order to avoid interfering interactions from the backbone atoms. The geometries of the two model complexes as well as each monomer were optimized at the M06-2X/6-311+G(d,p)[13, 14] level of theory, using Gaussian09[15]. A dielectric constant (ε=20) was used to mimic the rest of the environment; this choice was based upon the fact that this active site is close to the edge of the protein, rather than in the center[16]. Subsequent single point calculations using the SMD implicit model solvation (ε=20) were performed at the M06-2X/6-311+G(d,p) level and at the CCSD(T)/6-31+G(d,p)[17] level to obtain the energies of the complexes and monomers. The interaction energy for the H-bond was obtained as followed:

$$E_{H-Bond} = E_{complex} - E_{Cys} - E_{Thr/His}$$

For the CCSD(T)/6-31+G(d,p) level, the electronic energies were used; whereas for the M06-2X/6-311+G(d,p) level, the ZPVE-corrected electronic energies were used.

The interactions energies for the H-bonds for Cys-Thr and Cys-His complexes are collected in Table S1.

Table S1: The H-bond interaction energies (in kcal/mol) for the Cys-Thr and Cys-His complexes

Complex	M06-2X/6-311+G(d,p)	CCSD(T)/6-31+G(d,p)
Cys – Thr	-28.3	-35.1
Cys – His	-32.1	-41.4

Details of the pKa determination

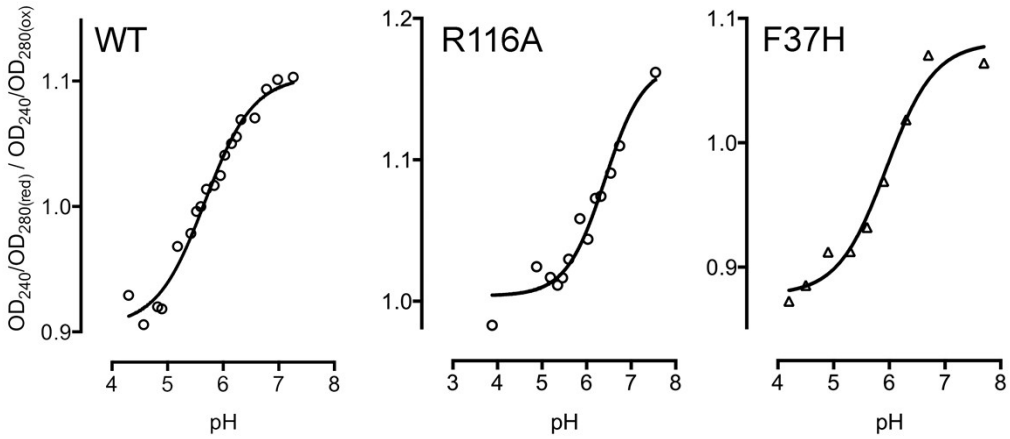

Figure S1: The pK_a determination of the C_P in the MtAhpE variants. The absorption $(A_{240}/A_{280})_{red}/(A_{240}/A_{280})_{ox}$ was plotted in function of the pH. The curves were fitted with the Henderson-Hasselbalch equation to determine the pK_a from the inflection point of the curve.

Details of the stopped-flow/kinetic measurements

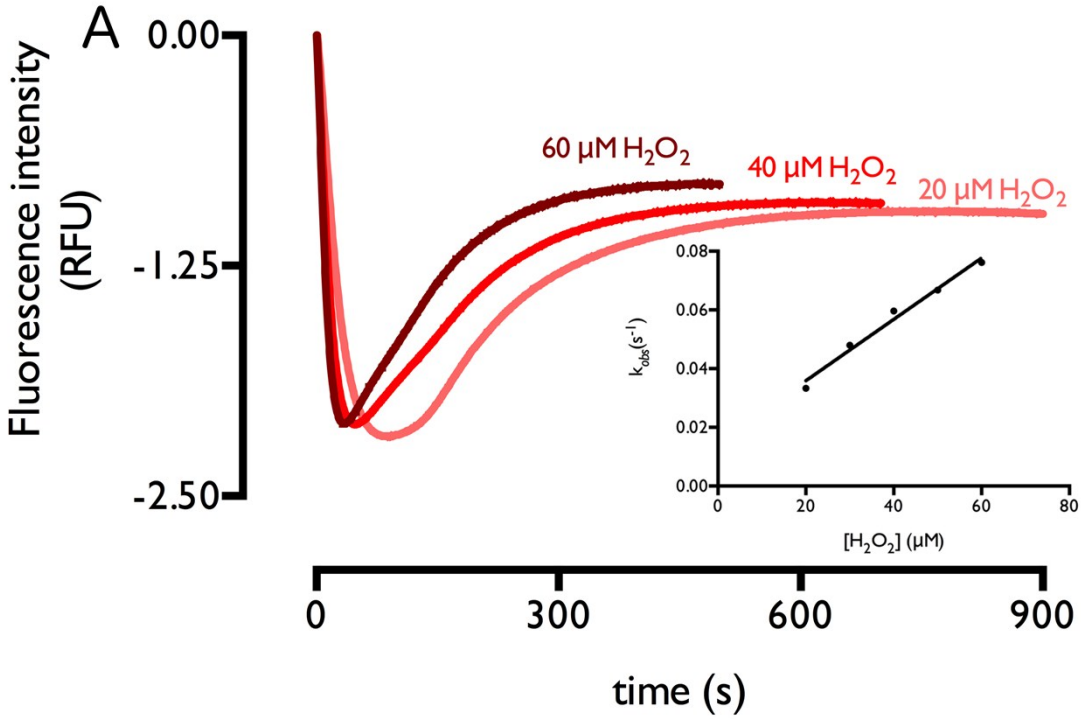

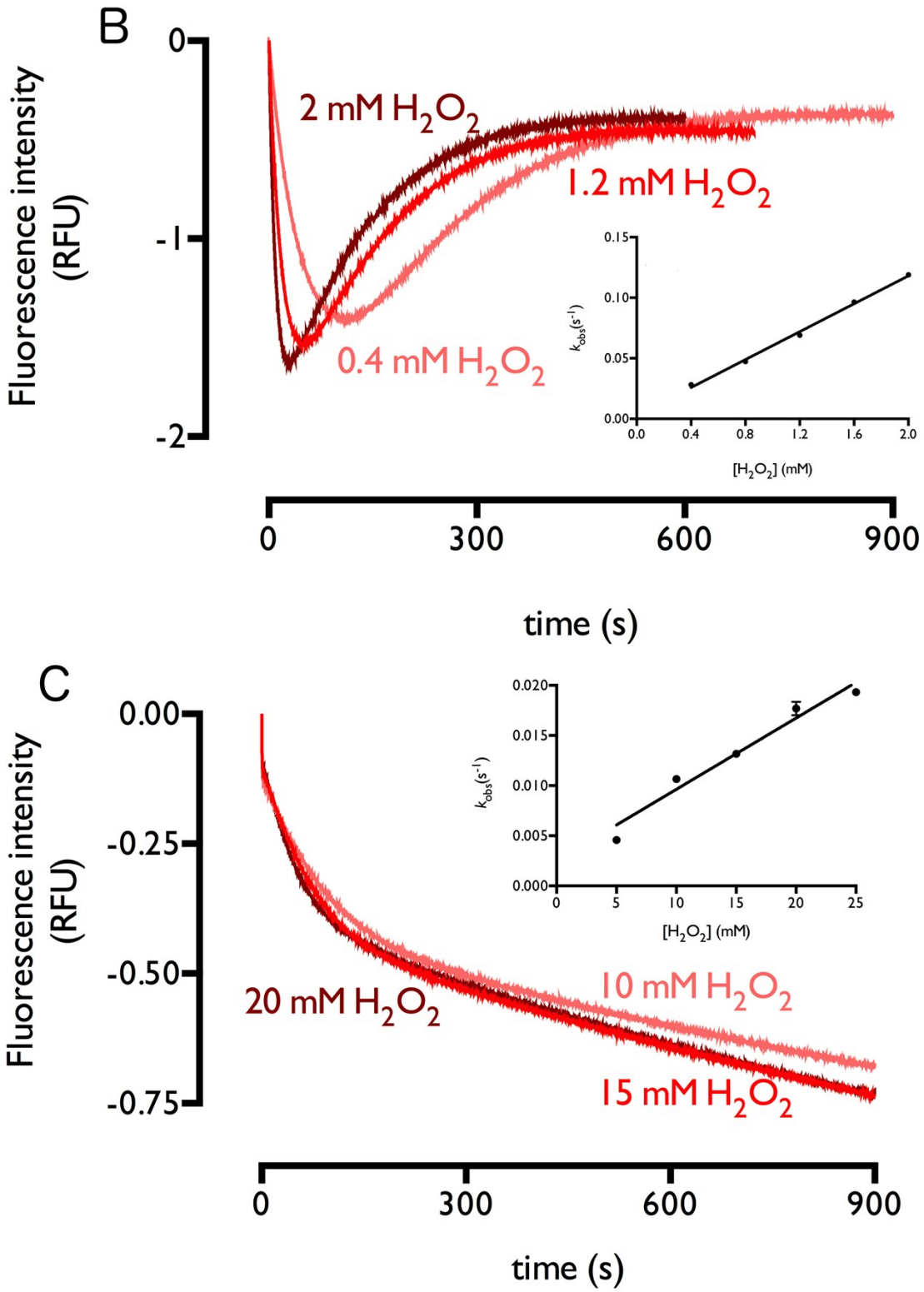

Figure S2: Progress curves of the F37H (A), T42V (B) and R116A (C) MtAhpE intrinsic fluorescence intensity upon enzyme oxidation by H_2O_2. Inset: Rate constant determination of the MtAhpE oxidation by H_2O_2, by determination of the linear relationship between the H_2O_2 concentration and the observed rate constant (k_{obs}). The progress curves show the result of one technical replicate, whereas the insets correspond to the average of three technical replicates.

Details of the crystallographic data

Table S2: Crystallization, data collection and refinement statistics

PDB Code	4XIH	5C04
Data Collection		
Wavelength (Å)	0.9763	0.980
Crystal to detector distance (mm)	353.9	300
Rotation range per image (˚)	0.15	0.2
Total rotation range (˚)	119.1	180
Data processing		
Space group	*I*4	$P4_32_12$
Cell constants (Å)	174.26 147.26 33.30	63.30 63.30 159.45
Resolution range	104-2.25	44.76-1.45
last shell	2.31-2.25	1.49-1.45
Mosaicity	0.153	0.053
Completeness (%)	97.8 (91.1)	97.8 (81.5)
No. of observed/unique	74914/17072	669845/57365
(last shell)	(10654/2575)	(21860/3472)
Redundancy (last shell)	4.38 (4.14)	11.67 (6.29)
Mean $I/\sigma(I)$	11.05 (1.92)	18.54 (1.88)
$R_{r.i.m.}$	0.114 (0.864)	0.077 (0.96)
Overall B-factor from Wilson plot (Å^2)	43.8	30.8
Optical resolution (Å)	1.74	1.38
Solvent content (%)	49	47
Refinement		
No. of reflections, working set	16096 (1100)	52091 (1615)
No. of reflections, test set	962 (54)	3432 (114)
R_{cryst}	0.210	0.166
R_{free}	0.224	0.198
DPI	0.302	0.062
Number of atoms		
protein	2393	2455
water molecules	61	167
R.m.s. deviations		
bonds (Å)	0.045	0.103
angles (˚)	1.2	1.43
Average B-factors (Å^2)		
protein	33.4	18.7
water molecules	38.1	33.8
Ramachandran plot		
favored (%)	96.1	97.8
allowed (%)	3.2	2.2

Supplemental references

1. M. Hugo, L. Turell, B. Manta, H. Botti, G. Monteiro, L. E. Netto, B. Alvarez, R. Radi and M. Trujillo, *Biochemistry*, 2009, **48**, 9416-9426.
2. G. Roos, A. Garcia-Pino, K. Van Belle, E. Brosens, K. Wahni, G. Vandenbussche, L. Wyns, R. Loris and J. Messens, *Journal of molecular biology*, 2007, **368**, 800-811.
3. W. Kabsch, *Acta crystallographica. Section D, Biological crystallography*, 2010, **66**, 125-132.
4. A. J. McCoy, R. W. Grosse-Kunstleve, P. D. Adams, M. D. Winn, L. C. Storoni and R. J. Read, *Journal of applied crystallography*, 2007, **40**, 658-674.
5. G. N. Murshudov, A. A. Vagin and E. J. Dodson, *Acta crystallographica. Section D, Biological crystallography*, 1997, **53**, 240-255.
6. P. Emsley and K. Cowtan, *Acta crystallographica. Section D, Biological crystallography*, 2004, **60**, 2126-2132.
7. V. B. Chen, W. B. Arendall, 3rd, J. J. Headd, D. A. Keedy, R. M. Immormino, G. J. Kapral, L. W. Murray, J. S. Richardson and D. C. Richardson, *Acta crystallographica. Section D, Biological crystallography*, 2010, **66**, 12-21.
8. B. R. Brooks, C. L. Brooks, 3rd, A. D. Mackerell, Jr., L. Nilsson, R. J. Petrella, B. Roux, Y. Won, G. Archontis, C. Bartels, S. Boresch, A. Caflisch, L. Caves, Q. Cui, A. R. Dinner, M. Feig, S. Fischer, J. Gao, M. Hodoscek, W. Im, K. Kuczera, T. Lazaridis, J. Ma, V. Ovchinnikov, E. Paci, R. W. Pastor, C. B. Post, J. Z. Pu, M. Schaefer, B. Tidor, R. M. Venable, H. L. Woodcock, X. Wu, W. Yang, D. M. York and M. Karplus, *Journal of computational chemistry*, 2009, **30**, 1545-1614.
9. A. D. MacKerell, D. Bashford, M. Bellott, R. L. Dunbrack, J. D. Evanseck, M. J. Field, S. Fischer, J. Gao, H. Guo, S. Ha, D. Joseph-McCarthy, L. Kuchnir, K. Kuczera, F. T. Lau, C. Mattos, S. Michnick, T. Ngo, D. T. Nguyen, B. Prodhom, W. E. Reiher, B. Roux, M. Schlenkrich, J. C. Smith, R. Stote, J. Straub, M. Watanabe, J. Wiorkiewicz-Kuczera, D. Yin and M. Karplus, *The journal of physical chemistry. B*, 1998, **102**, 3586-3616.
10. W. L. Jorgensen, J. Chandrasekhar, J. D. Madura, R. W. Impey and M. L. Klein, *J Chem Phys*, 1983, **79**, 926-935.
11. C. L. Brooks and M. Karplus, *J Chem Phys*, 1983, **79**, 6312-6325.
12. J. P. Ryckaert, G. Ciccotti and H. J. C. Berendsen, *J Comput Phys*, 1977, **23**, 327-341.
13. Y. Zhao and D. G. Truhlar, *Theoretical Chemistry Accounts*, 2008, **120**, 215-241.
14. W. J. Hehre, *Ab initio molecular orbital theory*, Wiley-Interscience, 1986.
15. M. Frisch, G. Trucks, H. Schlegel, G. Scuseria, M. Robb, J. Cheeseman, G. Scalmani, V. Barone, B. Mennucci and G. Petersson, *Gaussian 09, Revision B. 01. Gaussian, Inc., Wallingford, CT* 2010.
16. L. Li, C. Li, Z. Zhang and E. Alexov, *J Chem Theory Comput*, 2013, **9**, 2126-2136.
17. K. Raghavachari, G. W. Trucks, J. A. Pople and M. Head-Gordon, *Chemical Physics Letters*, 1989, **157**, 479-483.